Syntheses, Crystal Structures, and Electrochemical Properties of Binuclear Copper(II,II) $[Cu_2L^1Cl_2][ClO_4]_2·4CH_3CN$ and Copper(I,I) $[Cu_2L^1][ClO_4]_2$ Complexes {L^1 = 2,5-Bis[*N,N*-bis(2′-pyridylethyl)aminomethyl]pyrazine} *

Hiroki Oshio
Department of Applied Molecular Science, Institute for Molecular Science, Okazaki 444, Japan

---

The binuclear copper(II,II) and copper(I,I) complexes $[Cu_2L^1Cl_2][ClO_4]_2·4CH_3CN$ (**1**) and $[Cu_2L^1][ClO_4]_2$ (**2**) {L^1 = 2,5-bis[*N,N*-bis(2′-pyridylethyl)aminomethyl]pyrazine} have been synthesized. Crystal structures of both complexes have been determined. Complex (**1**) crystallizes in the triclinic space group $P\bar{1}$ with a = 13.140(3), b = 13.541(4), c = 8.217(2) Å, α = 101.43(4), β = 87.44(3), γ = 117.50(2)°, and Z = 1; complex (**2**) crystallizes in the triclinic space group $P\bar{1}$ with a = 10.264(6), b = 12.473(5), c = 9.213(2) Å, α = 89.92(2), β = 113.19(3), γ = 113.74(3)°, and Z = 1. The complex cations in (**1**) and (**2**) have centrosymmetric binuclear structures with copper atoms in distorted square pyramidal and pyramidal geometries respectively. E.s.r. and magnetic susceptibility data of (**1**) show the absence of a strong magnetic interaction between the copper atoms. In acetonitrile complex (**1**) shows a quasi-reversible cyclic voltammogram with E_{p_c} and E_{p_a} values at −0.09 and 0.06 V *vs.* Ag–AgCl. Controlled-potential electrolysis upon complex (**1**) demonstrates that the process involves the transfer of two electrons. The two-step reduction potentials leading to Cu^{II}–Cu^{I} and Cu^{I}–Cu^{I} from Cu^{II}–Cu^{II} were estimated to be at 0.04 and −0.07 V, respectively.

Binuclear copper sites are common in biological systems.[1,2] In haemocyanin for example, in which three imidazole ligands from histidine bind to a dicopper(I) site,[3] reversible uptake of O_2 is observed to occur, leading to a peroxodicopper(II) complex.[4] Central to this behaviour is the ready accessibility of both the copper-(I) and -(II) oxidation states.[5,6] Therefore an understanding of factors controlling the oxidation states of copper, particularly in terms of ligand design has been of continuing interest in co-ordination chemistry.

In a previous paper[7] the synthesis, structure, and electrochemical properties of the pyrazine-bridged binuclear Cu^{II} complex $[Cu_2L^2Cl_2][ClO_4]_2$ {L^2 = 2,5-bis[*N,N*-bis(2′-pyridylmethyl)aminomethyl]pyrazine} were reported. A two-step reduction process of this complex leading to Cu^{II}–Cu^{I} and Cu^{I}–Cu^{I} from Cu^{II}–Cu^{II} were observed with redox potentials estimated to be at −0.14 and −0.26 V *vs.* Ag–AgCl, respectively. Owing to the differing stereochemical preferences of Cu^{II} (square pyramidal, trigonal bipyramidal or intermediate between these two geometries), relative to Cu^{I} (tetrahedral or pyramidal), ready interconversion of these two oxidation states is facilitated by use of flexible ligands which can adjust their co-ordination geometry to the differing demands of the two oxidation states. In such cases it is possible to prepare both Cu^{II} and Cu^{I} complexes with the same ligand. In this study the aim was to synthesize a pyrazine-bridged binuclear copper(II,II) complex from which the Cu^{I} state would be more accessible than from $[Cu_2L^2Cl_2][ClO_4]_2$, by modification of the bridging ligand. Herein are reported the syntheses, crystal structures, magnetic and electrochemical properties of the pyrazine-bridged binuclear copper(II,II) complex $[Cu_2L^1Cl_2][ClO_4]_2·4CH_3CN$ and of the related copper(I,I) complex $[Cu_2L^1][ClO_4]_2$ {L^1 = 2,5-bis[*N,N*-bis(2′-pyridylethyl)aminomethyl]pyrazine}.

Experimental

Syntheses.—*2,5-Bis*[N,N-*bis*(*2′-pyridylethyl*)*aminomethyl*]*pyrazine* (L^1). A mixture of *N,N*-bis(2-pyridylethyl)amine (0.2 g, 0.51 mmol) (prepared from reaction of 2-aminoethylpyridine and 2-vinylpyridine) and Na_2CO_3 (0.53 g, 5 mmol) in freshly distilled acetonitrile (300 cm^3) was heated to reflux and a solution of 2,5-bis(bromomethyl)pyrazine[7] in acetonitrile (100 cm^3) was added dropwise within 2 h with stirring followed by refluxing for a further 6 h. After cooling to room temperature, the insoluble solid was filtered off and the filtrate was evaporated to dryness. The crude product was redissolved in $CHCl_3$ and purified on an alumina column with $CHCl_3$–MeOH (92:8) as eluant (3.3 g, 30% yield).

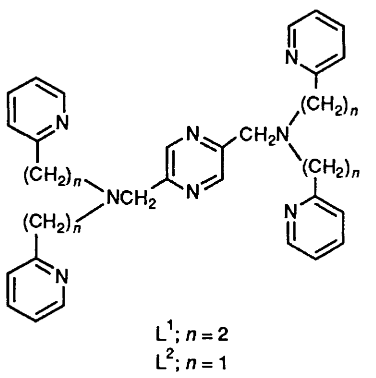

$[Cu_2L^1Cl_2][ClO_4]_2$. Sodium perchlorate (240 mg, 2 mmol) in MeOH (40 cm^3) was added to a mixture of L^1 (559 mg, 1 mmol) and $CuCl_2·4H_2O$ (340 mg, 2 mmol) also in MeOH (40 cm^3). The blue precipitate was filtered off, washed with cold MeOH, and dried *in vacuo* (Found: C, 42.75; H, 4.15; N, 11.75. $C_{34}H_{38}Cl_4Cu_2N_8O_8$ requires C, 42.75; H, 4.00; N, 11.75%).

$[Cu_2L^1][ClO_4]_2$. All procedures were performed under an

---

* *Supplementary data available* (No. SUP 56787, 2 pp.): variable temperature magnetic susceptibility data for complex (**1**). See Instructions for Authors, *J. Chem. Soc., Dalton Trans.*, 1990, Issue 1, pp. xix—xxii.

argon atmosphere. The compound $Cu(ClO_4)_2 \cdot 6H_2O$ (741 mg, 2 mmol) was added to an acetonitrile solution (50 cm^3) of L^1 (559 mg, 1 mmol). Copper powder (125 mg, 2 mmol) was added to this solution which turned from blue to red upon refluxing for 1 h. The solution was then filtered and the filtrate was stored in a refrigerator overnight. The red precipitate which formed was filtered off, washed with acetonitrile and dried *in vacuo* (Found: C, 46.30; H, 4.25; N, 12.50. $C_{34}H_{38}Cl_2Cu_2N_8O_8$ requires C, 46.15; H, 4.35; N, 12.65%).

Crystal Growth.—Slow evaporation of acetonitrile solutions over a slow stream of nitrogen gave blue (**1**) and red (**2**) tablets. Crystals of (**1**) contain four acetonitrile solvent molecules per cation which were readily lost upon drying *in vacuo* resulting in a loss of crystallinity. Unfortunately, the biggest crystal of (**2**) (selected for the diffraction study) which could be grown was of dimensions 0.10 × 0.10 × 0.08 mm, so limiting the quality of the resulting data set.

Physical Measurements.—Electronic spectra were recorded on an Hitachi U-3400 spectrophotometer, e.s.r. spectra on a JEOL FE2XG, *X*-band (100-kHz field modulation) spectrometer. The microwave frequency was measured with a Takeda Riken 5201 frequency counter and the magnetic field values of the signals were measured with an Echo Denshi EFM 2000. Magnetic susceptibility on powdered samples was measured by an Oxford Faraday-type magnetic balance system equipped with a superconducting magnet. Temperature readings were calibrated with a magnetic thermometer by the use of $[Cr(NH_3)_6]Cl_3$. Cyclic voltammetry (c.v.) and constant-potential electrolysis (c.p.e.) were accomplished with a three-electrode potentiostat (Hokuto Denko HA501G potentiostat/galvanostat and HB-105 function generator, and HA-105 potentiostat/galvanostat and HF201 digital coulometer, respectively). Internal resistance drop was compensated with a Hokuto HI-203 IR compensation instrument for c.v. The electrochemical measurements were performed at 25 °C by the use of a normal three-electrode configuration consisting of a highly polished glassy carbon working electrode (area 0.28 cm^3; BAS Ltd.), a platinum-wire auxiliary electrode, and an Ag–AgCl reference electrode containing 3 mol dm^{-3} NaCl solution (BAS Ltd.) in a micro-cell (BAS Ltd.). A platinum mesh for both working and auxiliary electrodes was used for c.p.e. The working and auxiliary compartments contained a 0.1 mol dm^{-3} solution of the supporting electrolyte. Spectral grade acetonitrile (Dojin Lab.) was used without further purification. The supporting electrolyte NEt_4PF_6 (Fluka Chemie AG Industries) was recrystallized two times from ethanol and water, and dried under vacuum in an oven at 80 °C for 10 h. The compartment of the cell was bubbled with solvent-saturated argon to deaerate the solution. Ferrocene was used as an internal standard. The correction employed an $E^{0\prime}$ value for the ferrocene–ferrocenium couple of 0.400 V *vs.* a normal hydrogen electrode (n.h.e.),[8] which was assumed to be independent of the solvent. Potentials for compounds are reported *vs.* corrected Ag–AgCl(aq). The potential of the ferrocene–ferrocenium was measured under the conditions employed: $CH_3CN–NEt_4PF_6$, $E^{0\prime} = 0.420$ V.

Crystallography.—*Crystal data.* Blue crystals of $[Cu_2L^1Cl_2][ClO_4]_2 \cdot 4CH_3CN$ (**1**). $C_{42}H_{50}Cl_4Cu_2N_{12}O_8$, $M = 1\,119.847$, triclinic, space group $P\bar{1}$, $a = 13.140(3)$, $b = 13.541(4)$, $c = 8.217(2)$ Å, $\alpha = 101.43(4)$, $\beta = 87.44(3)$, $\gamma = 117.50(2)°$, $U = 1\,269.2(6)$ Å^3, $Z = 1$, $D_c = 1.465$ g cm^{-3}, μ(Mo-K_α) = 11.437 cm^{-1}, λ(Mo-K_α) = 0.710 73 Å.

Red crystals of $[Cu_2L^1][ClO_4]_2$ (**2**). $C_{34}H_{38}Cl_2Cu_2N_8O_8$, $M = 884.721$, triclinic, space group $P\bar{1}$, $a = 10.264(6)$, $b = 12.473(5)$, $c = 9.213(2)$ Å, $\alpha = 89.92(2)$, $\beta = 113.19(3)$, $\gamma = 113.74(3)°$, $U = 975.0(9)$ Å^3, $Z = 1$, $D_c = 1.507$ g cm^{-3}, μ(Cu-K_α) = 31.349 cm^{-1}, λ(Cu-K_α) = 1.541 78 Å.

Data collection and processing. Intensity data were collected at room temperature with crystals [0.56 × 0.28 × 0.10 mm for (**1**) and 0.10 × 0.10 × 0.08 mm for (**2**)] on Rigaku AFC-5 and Enraf-Nonius CAD-4 four-circle diffractometers respectively by use of the ω—2θ scan technique and graphite monochromated Mo-K_α and Cu-K_α radiation, respectively: 9 734 ($2 < 2\theta < 65°$; $-19 < h < 19$, $-20 < k < 20$, $0 < l < 12$) and 2 890 reflections ($2 < 2\theta < 120°$; $-10 < h < 10$, $-11 < k < 11$, $0 < l < 14$) were measured for (**1**) and (**2**), of which 6 200 and 611 were observed [$|F_o| > 3\sigma(F_o)$] and [$|F_o| > 4\sigma(F_o)$], respectively. The intensities were corrected for Lorentz and polarization factors and absorption, but not for extinction. Lattice constants were determined by a least-squares refinement based on 50 reflections [$13 < \theta < 15°$ and $10 < \theta < 15°$ for (**1**) and (**2**), respectively] measured on the diffractometers.

Structure analysis and refinement. The structures were solved by the conventional heavy-atom method and refined by a block-diagonal least-squares technique with anisotropic thermal parameters for non-H atoms and isotropic for H atoms for (**1**). In the structure analysis of (**1**), a rotational disorder of the perchlorate anion around Cl–O(1) was observed and the positional and anisotropic thermal parameters of the disordered oxygen atoms were included in the refinement. As stated before, large crystals of (**2**) could not be grown, and only 611 reflections were available for the refinement. Its structure was refined with anisotropic thermal parameters for copper and chlorine atoms only and isotropic for other atoms, and the hydrogen atoms were not included in the refinement. Atomic scattering factors and anomalous scattering corrections were taken from ref. 9. In the refinements, weighting schemes $w = [\sigma^2_c + (0.025|F_o|)^2]^{-1}$ and $w = [\sigma^2_c + (0.015|F_o|)^2]^{-1}$ for (**1**) and (**2**), respectively, were chosen where σ^2_c was the standard deviation of $|F_o|$ calculated from counting statistics. The final R and R' values were 0.048 and 0.058 for (**1**), and 0.099 and 0.096 for (**2**). Final atomic parameters for non-hydrogen atoms are listed in Tables 1 and 2.

All the calculations were carried out on a HITAC M680 computer at the Computer Center of the Institute for Molecular Science with the Universal Crystallographic Computation Program System UNICS-III.[10]

Additional material available from the Cambridge Crystallographic Data Centre comprises H-atom co-ordinates, thermal parameters, and remaining bond lengths and angles.

Results and Discussion

Description of the Structure.—Blue crystals of complex (**1**) consist of $[Cu_2L^1Cl_2]^{2+}$, ClO_4^- and acetonitrile molecules, while the red crystals of (**2**) contain $[Cu_2L^1]^{2+}$ and ClO_4^-. ORTEP drawings of the molecular structures of both complexes are presented in Figures 1 and 2, together with the atomic labelling system; the ClO_4^- anions and acetonitrile molecules for (**1**) are omitted for clarity. Selected bond lengths and angles are listed in Tables 3 and 4.

In complex (**1**) each Cu^{2+} is co-ordinated to four nitrogen atoms of the ligand (one N atom of pyrazine, one N atom of amine, and two N atoms of the pyridine moiety) and to a chlorine atom. Each of the two five-co-ordinated CuN_4Cl chromophores is related by a crystallographic centre of symmetry. The co-ordination geometry around each Cu atom in (**1**) is a distorted square pyramid. The angles Cl(1)–Cu–N(1) and N(2)–Cu–N(4) are 161.45(8) and 165.63(11)°, respectively, so the plane defined by Cl(1), N(1), N(2), and N(4) can be regarded as a basal plane of the square pyramid for complex (**1**). By using an index τ introduced by Addison *et al.*,[11] which is

Table 1. Fractional atomic co-ordinates (× 10^5 for Cu and × 10^4 for the other atoms) with estimated standard deviations (e.s.d.s) in parentheses for $[Cu_2L^1Cl_2][ClO_4]_2 \cdot 4CH_3CN$ (**1**)

Atoms	*x*	*y*	*z*
Cu	32 938(3)	21 929(2)	49 323(3)
Cl(1)	2 748(1)	2 542(1)	7 570(1)
N(1)	3 562(2)	2 208(2)	2 401(2)
N(2)	2 002(2)	610(2)	4 511(3)
N(3)	4 693(2)	1 805(2)	5 401(3)
N(4)	4 320(2)	3 879(2)	5 084(2)
C(1)	2 577(3)	1 297(2)	1 250(3)
C(2)	1 434(3)	981(2)	2 013(4)
C(3)	1 219(2)	214(2)	3 228(3)
C(4)	278(3)	−853(2)	3 036(4)
C(5)	142(3)	−1 535(2)	4 162(4)
C(6)	946(3)	−1 132(2)	5 463(4)
C(7)	1 858(2)	−58(2)	5 606(3)
C(8)	4 644(3)	2 149(2)	1 926(3)
C(9)	4 755(3)	1 173(3)	2 423(4)
C(10)	5 230(2)	1 431(2)	4 178(3)
C(11)	6 169(3)	1 295(3)	4 531(4)
C(12)	6 569(3)	1 528(3)	6 152(4)
C(13)	6 024(3)	1 905(3)	7 408(4)
C(14)	5 101(2)	2 030(3)	6 975(3)
C(15)	3 695(2)	3 330(2)	2 199(3)
C(16)	4 410(2)	4 225(2)	3 644(3)
C(17)	4 907(2)	4 645(2)	6 444(3)
C(S1)*	8 344(4)	5 431(5)	1 061(8)
C(S2)*	7 141(4)	4 886(3)	357(5)
N(S1)*	6 234(3)	4 479(3)	−172(5)
C(S3)*	8 848(6)	4 376(5)	6 406(9)
C(S4)*	8 294(6)	4 963(8)	5 932(9)
N(S2)*	7 944(8)	5 530(10)	5 619(10)
Cl(2)	1 521(1)	−2 316(1)	−716(1)
O(1)	1 288(4)	−2 843(4)	654(5)
O(2)	1 436(7)	−2 945(5)	−2 254(7)
O(3)	2 582(6)	−1 351(5)	−274(10)
O(4)	683(6)	−1 854(7)	−742(8)
O(2′)	2 199(10)	−1 217(6)	−816(11)
O(3′)	2 256(14)	−2 816(11)	−1 580(15)
O(4′)	608(11)	−2 820(10)	−1 662(17)

* S denotes a solvent atom.

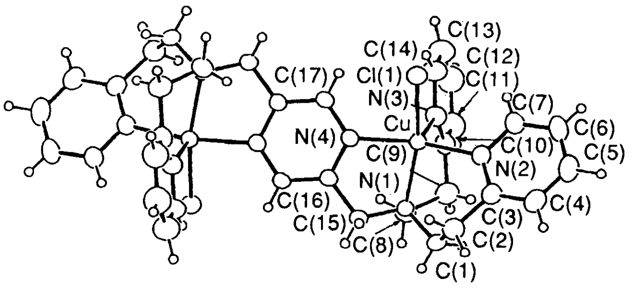

Figure 1. Molecular structure of $[Cu_2L^1Cl_2]^{2+}$ (**1**). Thermal ellipsoids are drawn at the 50% probability level

defined as [N(2)–Cu–N(4) − Cl(1)–Cu–N(1)/60°] in this system, it is possible to elucidate whether the geometry is square pyramidal, trigonal bipyramidal, or intermediate between these two geometries. The index τ is unity for a perfect trigonal bipyramid and zero for a square pyramid. The calculated τ value for (**1**) is 0.07, that is the geometry of the copper ion is very close to square pyramidal. Displacement of the copper atom from the best-fit basal plane [Cl(1)–N(1)–N(2)–N(4)] is 0.293(1) Å. The dihedral angle between this basal plane and the pyrazine ring is 26.4(1)°. The co-ordination bond lengths at copper [1.999(2)—2.200(3) for Cu–N and 2.281(1) Å for Cu–Cl] are a little shorter than those for $[Cu_2L^2Cl_2][ClO_4]_2$[2.011—2.257(3) for Cu–N and 2.233(1) Å for Cu–Cl] in which the geometry around the copper atom is not as close (τ = 0.44) to a perfect square pyramid as in complex (**1**).[7]

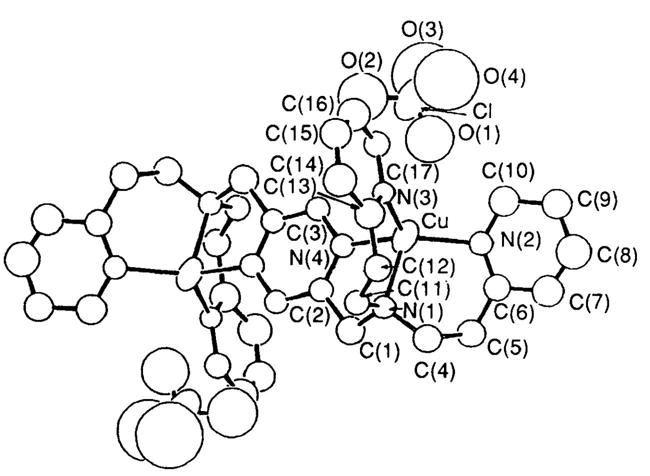

Figure 2. Molecular structure of $[Cu_2L^1][ClO_4]_2$ (**2**). Thermal ellipsoids are drawn at the 50% probability level

In complex (**2**) each Cu^I ion is four-co-ordinate with the two CuN_4 chromophores related by a crystallographic inversion centre. The Cu–N bond lengths lie within a relatively narrow range [2.03(3)—2.17(3) Å], but the angles (NCuN) around the copper atoms show a wide variation [83.6(10)—140.3(9)°]. In the solid state the stereochemistry of Cu^I is dominated by four-co-ordination and can be classified into four types, *viz*., tetrahedral, trigonal-pyramidal, see-saw, and square co-planar geometries.[12] Noting the wide variation in the angles around the copper atom above, with the largest falling well short of the 180° characteristic of see-saw geometry, the co-ordination about Cu^I is best described as trigonal pyramidal with the Cu atom displaced from a tetrahedral position towards the plane containing atoms N(2), N(3), and N(4). In the solid state the space opposite to the Cu–N(1) bond seems to be associated with perchlorate ion, and there might be an electrostatic interaction between copper and perchlorate oxygen atoms [Cu–O(1) 3.56(4) Å]. Intramolecular copper–copper separations are 6.793(2) and 6.743(7) Å for complexes (**1**) and (**2**), respectively.

Electronic and Magnetic Properties.—Structural studies concerning the electronic configuration of copper have been performed for mononuclear Cu^{II} compounds with tripod ligands[13–15] and a series of $[Cu(bipy)_2X]^+$ (bipy = 2,2′-bipyridine) cations.[16–18] The electronic spectrum [Figure 3(*a*)] of $[Cu_2L^1Cl_2][ClO_4]_2$ (**1**) in acetonitrile has a band maximum at 655 nm (ε = 467 $dm^3 mol^{-1} cm^{-1}$), while no *d–d* transition band was observed for $[Cu_2L^1][ClO_4]_2$ (**2**) [Figure 3(*b*)]. Electronic spectra of copper(II) complexes with trigonal-bipyramidal and square-pyramidal geometries have been studied extensively by Hathaway and co-workers,[19] and by reference to this the band at 655 nm for complex (**1**) can be assigned to the $d_{xz},d_{yz} \longrightarrow d_{x^2-y^2}$ transition for a square-pyramidal system.

E.s.r. spectra of five-co-ordinate copper(II) complexes show characteristic patterns depending on the stereochemistry of the Cu^{II} centre.[20] An e.s.r. spectrum (Figure 4) of a powdered sample of complex (**1**) at 297 K indicates axial symmetry ($g_\perp$ = 2.076 and $g_\parallel$ = 2.200) and with no $\Delta M = 2$ transition around 1 600 G (0.16 Tesla) even at liquid-nitrogen temperature. The spectrum can be accounted for by a $d_{x^2-y^2}$ ground state of the copper atom with square-pyramidal geometry in accord

Table 2. Fractional atomic co-ordinates (× 10^4 for Cu and Cl atoms and × 10^3 for the other atoms) with e.s.d.s in parentheses for $[Cu_2L^1][ClO_4]_2$ (**2**)

Atom	*x*	*y*	*z*
Cu	1 572(6)	6 855(5)	8 520(6)
Cl	−2 852(19)	7 504(17)	6 213(16)
N(1)	327(3)	613(2)	903(3)
N(2)	150(3)	701(2)	1 067(2)
N(3)	280(2)	848(2)	804(2)
N(4)	42(3)	568(2)	637(3)
C(1)	243(4)	493(3)	793(4)
C(2)	117(3)	500(2)	635(3)
C(3)	−73(3)	574(2)	500(3)
C(4)	390(4)	597(3)	1 072(4)
C(5)	257(4)	550(3)	1 144(4)
C(6)	213(3)	643(3)	1 168(3)
C(7)	246(4)	678(3)	1 330(4)
C(8)	203(4)	757(3)	1 358(4)
C(9)	124(4)	812(3)	1 249(4)
C(10)	89(4)	773(3)	1 082(4)
C(11)	456(3)	685(3)	866(3)
C(12)	530(4)	818(3)	930(4)
C(13)	439(4)	885(3)	834(4)
C(14)	499(4)	983(3)	747(4)
C(15)	403(4)	1 032(3)	668(4)
C(16)	260(4)	1 001(3)	655(4)
C(17)	178(3)	896(3)	714(3)
O(1)	−202(4)	713(3)	723(4)
O(2)	−266(4)	740(3)	485(4)
O(3)	−389(6)	753(5)	601(6)
O(4)	−198(6)	857(5)	739(6)

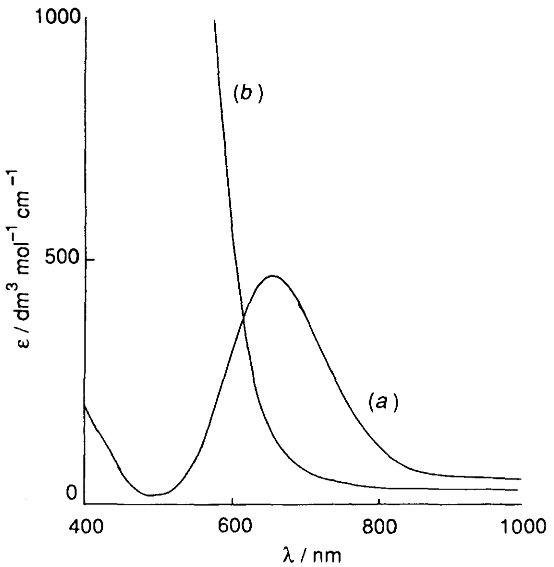

Figure 3. Electronic spectra of (*a*) $[Cu_2L^1Cl_2]^{2+}$ (**1**) and (*b*) $[Cu_2L^1]^{2+}$ (**2**) in acetonitrile

Table 3. Selected bond lengths (Å) and angles (°) with e.s.d.s in parentheses for $[Cu_2L^1Cl_2][ClO_4]_2 \cdot 4CH_3CN$ (**1**)

Cu–Cl(1)	2.281(1)	Cu–N(1)	2.097(2)
Cu–N(2)	1.999(2)	Cu–N(3)	2.200(3)
Cu–N(4)	2.026(2)	Cu ··· Cu*	6.793(2)
Cl(1)–Cu–N(1)	161.45(8)	Cl(1)–Cu–N(2)	91.06(8)
Cl(1)–Cu–N(3)	100.96(6)	Cl(1)–Cu–N(4)	90.27(7)
N(1)–Cu–N(2)	93.93(9)	N(1)–Cu–N(3)	95.96(10)
N(1)–Cu–N(4)	80.59(9)	N(2)–Cu–N(3)	98.52(10)
N(2)–Cu–N(4)	165.63(11)	N(3)–Cu–N(4)	95.27(9)

* Symmetry operation: 1 − *x*, 1 − *y*, 1 − *z*.

Table 4. Selected bond lengths (Å) and angles (°) with e.s.d.s in parentheses for $[Cu_2L^1][ClO_4]_2$ (**2**)

Cu–N(1)	2.17(3)	Cu–N(2)	2.03(3)
Cu–N(3)	2.07(2)	Cu–N(4)	2.06(2)
Cu–O(1)	3.56(4)	Cu ··· Cu*	6.743(7)
N(1)–Cu–N(2)	101.6(10)	N(1)–Cu–N(3)	99.5(10)
N(1)–Cu–N(4)	83.6(10)	N(2)–Cu–N(3)	112.7(9)
N(2)–Cu–N(4)	140.3(9)	N(3)–Cu–N(4)	105.0(9)

* Symmetry operation: 1 − *x*, 1 − *y*, 1 − *z*.

with the electronic spectrum observed. The temperature dependence of the magnetic susceptibility for (**1**) in the temperature range 4.5—230 K was measured. The data (SUP 56787) obey the Curie–Weiss law and the Curie and Weiss constants were estimated to be 0.448 cm^3 K mol^{-1} and −3.6 K respectively. Both the e.s.r. and magnetic susceptibility data show the absence of a strong magnetic interaction between the two copper atoms. Weak intramolecular antiferromagnetic interactions have been observed, however, for other pyrazine bridged binuclear Cu^{II} systems $J = -1.7$ cm^{-1} for $[Cu_2(dapz)(dien)_2][ClO_4]_4$[21] {dapz = 2,5-bis[(dimethylamino)methyl]pyrazine and dien = diethylenetriamine}; $J = -3.2$ cm^{-1} for $[Cu_2(tren)_2(pyz)][ClO_4]_4$ [tren = tris(2-aminoethyl)amine and pyz = pyrazine].[22] It is important that the magnetic orbitals of the metal ion are directed towards the bridging ligand (in this instance the σ orbital of the pyrazine nitrogen) to enable overlap between them, and this requirement was satisfied in these two complexes. The apparent absence of an intramolecular magnetic interaction in complex (**1**) can be interpreted by mixing of the $d_{x^2-y^2}$ and d_{z^2} magnetic orbitals owing to displacement of the copper atom from the basal plane(distortion towards trigonal-bipyramidal geometry), which might cause a subtle overlap of metal based magnetic orbitals with σ orbitals of the bridging atom. A substantial energy difference between these d_{z^2} and σ orbitals might be also responsible for the failure to detect a magnetic exchange interaction.[23]

Electrochemistry.—The redox properties of $[Cu_2L^1Cl_2][ClO_4]_2$ (**1**) and $[Cu_2L^1][ClO_4]_2$ (**2**) were studied by cyclic voltammetry (c.v.) and controlled potential electrolysis (c.p.e.). The cyclic voltammogram [Figure 5(*a*)] for complex (**1**) in acetonitrile shows a quasi-reversible wave for which E_{p_c} and E_{p_c} are at −0.09 and 0.06 V *vs.* Ag–AgCl, respectively. Based on c.p.e. carried out at the cathodic peak potential (−0.12 V), this wave was shown to correspond to a two-electron transfer. The *d–d* transition band of (**1**) at 655 nm disappeared after the completion of c.p.e., indicating that both Cu^{II} atoms in the molecule were reduced to Cu^I. It is possible to estimate individual redox potentials [$E^1_{\frac{1}{2}}$ and $E^2_{\frac{1}{2}}$ in equation(1)] for multi-step electron-transfer processes using measured E_{p_c} and E_{p_a} values.[24–26]

$$Cu^{II}–Cu^{II} + e^- \xrightarrow{E^1_{\frac{1}{2}}} Cu^{II}–Cu^I + e^- \xrightarrow{E^2_{\frac{1}{2}}} Cu^I–Cu^I \quad (1)$$

If the cyclic voltammogram for two one-electron steps shows two separate peaks with a large $\Delta E_{\frac{1}{2}}$ (= $E^1_{\frac{1}{2}} - E^2_{\frac{1}{2}}$ > 250 mV) value, then $E^1_{\frac{1}{2}}$ and $E^2_{\frac{1}{2}}$ can be measured directly. On the other hand, in the case of a smaller $\Delta E_{\frac{1}{2}}$ value the wave is distorted

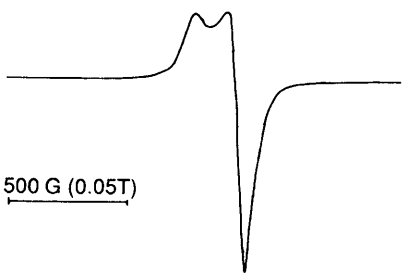

Figure 4. E.s.r. of powder spectra (*X*-band at 290 K) of $[Cu_2L^1Cl_2][ClO_4]_2$ (**1**)

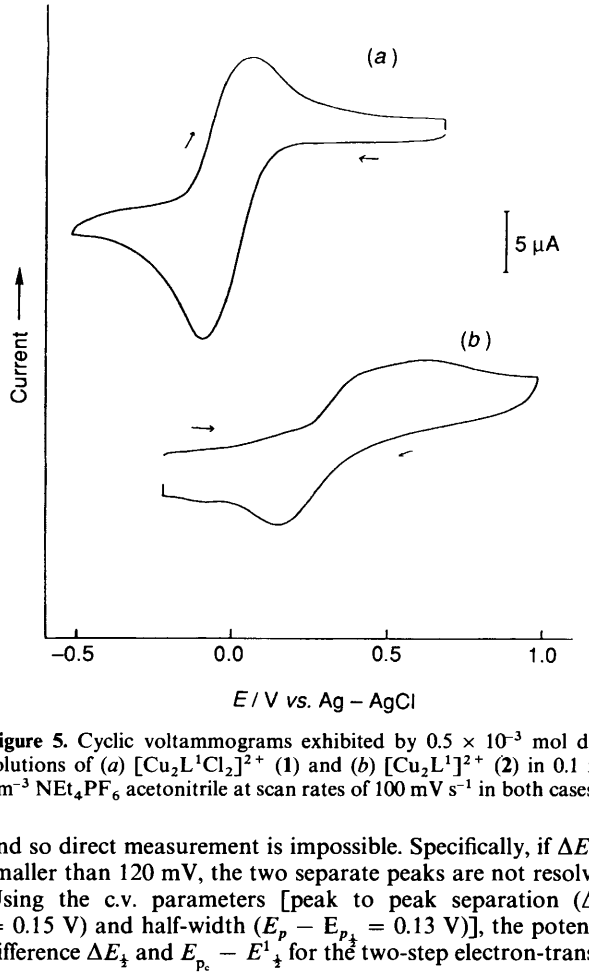

Figure 5. Cyclic voltammograms exhibited by 0.5 × 10^{-3} mol dm^{-3} solutions of (*a*) $[Cu_2L^1Cl_2]^{2+}$ (**1**) and (*b*) $[Cu_2L^1]^{2+}$ (**2**) in 0.1 mol dm^{-3} NEt_4PF_6 acetonitrile at scan rates of 100 mV s^{-1} in both cases

and so direct measurement is impossible. Specifically, if $\Delta E_{\frac{1}{2}}$ is smaller than 120 mV, the two separate peaks are not resolved. Using the c.v. parameters [peak to peak separation (ΔE_p = 0.15 V) and half-width ($E_p - E_{p_{\frac{1}{2}}}$ = 0.13 V)], the potential difference $\Delta E_{\frac{1}{2}}$ and $E_{p_c} - E^1_{\frac{1}{2}}$ for the two-step electron-transfer reaction are estimated to be 0.11 and −0.13 V, respectively.[24] Therefore, the $E^1_{\frac{1}{2}}$ and $E^2_{\frac{1}{2}}$ values are calculated to be 0.04 (= −0.09 + 0.13) and −0.07 V (= 0.04 − 0.11 V), respectively. It is interesting to compare these redox properties with the related complex $[Cu_2L^2Cl_2]^{2+}$.[7] Quasi-reversible two-step redox behaviour in acetonitrile was also observed for this complex and the corresponding redox potentials $E^1_{\frac{1}{2}}$ and $E^2_{\frac{1}{2}}$ were −0.14 and −0.26 V *vs.* Ag–AgCl, respectively. It should be noted that complex (**1**) is reduced more easily than $[Cu_2L^2Cl_2]^{2+}$, indicating that increased chelate ring size is the dominant factor in determining the stability of Cu^I relative to Cu^{II}. This result can be explained by the different stereochemistries adopted by Cu^I and Cu^{II} ions, as previously discussed. The ligand L^1 has two ethylene groups connecting each tertiary amine with a pyridine ring whilst in L^2 these are replaced by methylene groups. The more flexible ligand, L^1, is therefore more capable of modifying its co-ordination structure as the copper is reduced, and therefore complex (**1**) is reduced more easily than its L^2 analogue. This tendency has also been observed for mononuclear Cu^{II} complexes with tripodal ligands.[5] Cyclic voltammetry of complex (**2**) in acetonitrile shows only an irreversible wave [Figure 5(*b*)]. Controlled potential electrolysis at 0.6 V could not determine the number of electrons associated with this oxidation owing to further chemical reactions of the oxidized species. In complex (**1**), the co-ordinated chlorine atom may enable bond formation and breaking to occur more readily so enabling a redox process to occur and this might be responsible for the quasi-reversibility observed for complex (**1**). It is interesting to compare the redox behaviour of complex (**1**) with that of (**2**). Both E_{p_c} (0.4—0.6 V) and E_{p_a} (0.15 V) values for (**2**) are more positive than the $E^2_{\frac{1}{2}}$ value (0.04 V) for (**1**). In other words complex (**1**) is harder to reduce than the oxidized species of complex (**2**). This result might be explained by the fact that chlorine co-ordinates to the copper atom in complex (**1**), causing an increase in electron density on the copper atom and so making reduction more difficult than for the oxidized species of complex (**2**).

Acknowledgements

The author is grateful to Mr. Yoshihito Hayashi (Institute for Molecular Science) for the electrochemical measurements, and for financial support from the Ministry of Education, Science and Culture of Japan.

References

1 E. I. Solomon, 'Metal Ions in Biology,' ed. T. G. Spiro, Willey-Interscience, New York, 1981, vol. 3, p. 41.
2 E. I. Solomon, *Struct. Bonding (Berlin)*, 1983, **53**, 1.
3 W. P. J. Gaykema, W. G. J. Hol, J. M. Vereijken, N. M. Soerer, H. J. Bak, and J. J. Beintema, *Nature (London)*, 1984, **309**, 23.
4 M. S. Co, K. O. Hodgson, T. K. Eccles, and R. Lontie, *J. Am. Chem. Soc.*, 1981, **103**, 984.
5 K. D. Karlin and J. Zubieta (eds.), 'Copper Coordination Chemistry: Biochemical and Inorganic Perspectives,' Adenine Press, Guilderland, New York, 1983.
6 Z. Tyeklar and K. D. Karlin, *Acc. Chem. Res.*, 1989, **22**, 241.
7 H. Oshio, K. Toriumi, and Y. Hayashi, *J. Chem. Soc., Dalton Trans.*, 1990, 293.
8 H. M. Koepp, H. Wendt, and Z. Z. Strehlow, *Z. Elektrochem.*, 1960, **64**, 483.
9 'International Tables for *X*-Ray Crystallography,' Kynoch Press, Birmingham, 1974, vol. 4.
10 T. Sakurai and K. Kobayashi, *Rikagaku Kenkyusho Hokoku*, 1979, **55**, 69.
11 A. W. Addison, T. N. Rao, J. Reedijk, J. van Rijin, and G. C. Verschoor, *J. Chem. Soc., Dalton Trans.*, 1984, 1349.
12 B. J. Hathaway, in 'Comprehensive Coordination Chemistry,' eds. G. Wilkinson, R. D. Gillard, and J. A. McCleverty, Pergamon, Oxford, 1987, vol. 5, p. 539.
13 K. D. Karlin, J. C. Hayes, S. Juen, J. P. Hutchison, and J. Zubieta, *Inorg. Chem.*, 1982, **21**, 4106.
14 T. N. Sorrell and D. L. Jameson, *Inorg. Chem.*, 1982, **21**, 1014.
15 P. C. Jain and E. C. Lingafelter, *J. Am. Chem. Soc.*, 1967, **89**, 724.
16 S. Tyagi, B. Hathaway, S. Kremer, H. Stratemeier, and D. Reinen, *J. Chem. Soc., Dalton Trans.*, 1984, 2087.
17 W. D. Harrison, D. M. Kennedy, M. Power, R. Sheahan, and B. J. Hathaway, *J. Chem. Soc., Dalton Trans.*, 1981, 1556.
18 O. P. Anderson and A. B. Packard, *Inorg. Chem.*, 1980, **19**, 2941.
19 M. Duggan, N. Ray, and B. Hathaway, *J. Chem. Soc., Dalton Trans.*, 1980, 1342.
20 B. J. Hathaway, *Struct. Bonding (Berlin)*, 1984, **57**, 55.
21 H. Oshio and U. Nagashima, *Inorg. Chem.*, in the press.
22 M. S. Hadded, D. N. Hendrickson, J. P. Cannady, R. S. Drago, and D. S. Bieksza, *J. Am. Chem., Soc.*, 1979, **101**, 898.
23 M. S. Hadded and D. N. Hendrickson, *Inorg. Chem.*, 1978, **17**, 2622.
24 D. E. Richardson and H. Taube, *Inorg. Chem.*, 1981, **20**, 1278.
25 D. Polcyn and I. Shain, *Anal. Chem.*, 1966, **38**, 376.
26 R. L. Myers and I. Shain, *Anal. Chem.*, 1969, **41**, 980.

Received 5th *March* 1990; *Paper* 0/00987C